Dalton Transactions

Ferrocene Tethered Boramidinate Frustrated Lewis Pairs: Stepwise Capture of CO2 and CO

Journal:	*Dalton Transactions*
Manuscript ID	DT-ART-03-2022-000691.R1
Article Type:	Paper
Date Submitted by the Author:	17-Mar-2022
Complete List of Authors:	Esarte Palomero, Orhi; The university of Texas at Austin, Chemistry Jones, Richard; University of Texas at Austin, Department of Chemistry

ARTICLE

Ferrocene Tethered Boramidinate Frustrated Lewis Pairs: Stepwise Capture of CO_2 and CO

Received 00th January 20xx,
Accepted 00th January 20xx

DOI: 10.1039/x0xx00000x

Orhi Esarte Palomero[a] and Richard A. Jones*[a]

The synthesis and reactivity of novel ferrocene tethered boramidinate frustrated Lewis pairs (FLPs), capable of the sequential capture of small molecules, is reported. Reactions of 1,1'-dicarbodiimidoferrocenes with different boranes provides access to metallocene tethered FLPs. The reactivity of the boramidinate moieties can be tuned by the nature of the carbodiimido substituents (alkyl vs aryl) and the borane used in the reduction (9-borabicyclo[3.3.1]nonane $[(C_8H_{14})_2BH]_2$ vs. bis-pentafluorophenyl borane $[(C_6F_5)_2BH]_2$). The boramidinate FLP arms do not engage in intramolecular reactions, allowing for independent small molecule capture by each FLP. By careful synthetic control, sequential capture of different gaseous small molecules (CO_2 and CO or CO_2 and CNtBu) by the same bis(boramidinate)ferrocene molecule has been demonstrated.

Introduction

Frustrated Lewis pairs (FLPs) derived from main group elements have a promising potential for the transition metal (TM) free capture and utilization of small molecules.[1–4] To this date FLP chemistry and closely related main group Lewis acids and bases have been exploited for a variety of chemical transformations: (de)hydrogenation[5–7], hydrosilylation[8], hydroboration[9–12] or emerging new applications like nitrogen fixation[13,14] or polymer chemistry.[15–17]

Transition metals with their extended coordination sphere can flexibly accommodate diverse ligands and cycle through variable oxidation states during catalysis. In contrast, a single FLP can activate a wide range of small molecules but generally speaking the same FLP moiety can only activate one equivalent of a small molecule before being quenched (Scheme 1) (with some notable exceptions).[18–23] It would be desirable to design an FLP system capable of activating more than one substrate or functional group in order to perform more complex chemical transformations and extend the scope of FLP chemistry.[24–27] A more synthetically convenient alternative, given the now extensive literature on FLPs, would be the combination of two FLP moieties with known reactivity for small molecules in a tandem or bifunctional FLP system.[28–30] Within this same context tandem FLP/TM catalysis[31–33] and the reactivity of FLPs containing only TMs[34–39] have attracted recent interest.

The development of novel multifunctional FLP catalysts will require a fundamental understanding of how the FLP mediated small molecule activation is affected by several FLPs interacting in close proximity. In other studies, we have reported a series of bulky 1,1'-dicarbodiimidoferrocenes which can serve as heteroallylic pincer ligand precursors for early transition metals.[40] We hypothesized that we could repurpose this ligand scaffold to construct a multifunctional FLP model system by linking two boramidinate FLPs of recognized reactivity with a ferrocene linker. Boramidinates can be synthetized from the reaction of carbodiimides with boranes.[41] Their reactivity with CO, CO_2, isocyanides and other small molecules has been well stablished[42–44], primarily applied in the context of CO/CO_2 hydroboration using a variety of heteroallylic derivatives to support the borane.[45–52]

Herein, we report the synthesis of 1,1'-bis(boramidinate) ferrocene FLPs derived from the reaction of the 1,1'-dicarbodiimidoferrocene scaffold with 9-borabicyclo[3.3.1]nonane (9-BBN) (**2** & **4**) (Scheme 2) and bis-pentafluorophenyl borane $[(C_6F_5)_2BH]_2$ (**11**) (Scheme 5). The reactivity of these compounds towards CO, CO_2 and CNtBu was studied, ultimately leading to the sequential capture of CO and CO_2 (**17**) and of CO_2 and CNtBu (**19**) by the same molecule (**11**).

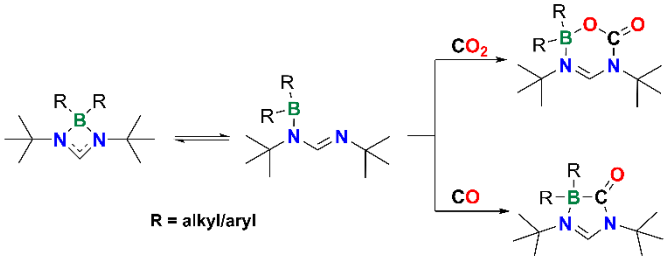

Scheme 1 Example of small molecule capture (CO and CO_2) by boramidinate based FLPs.[42]

[a] Department of Chemistry – The University of Texas at Austin
105 E 24th St, Austin, TX 78712, USA
E-mail: rajones@utexas.edu

Electronic Supplementary Information (ESI) available: CCDC 1969187-1969198, 2091566. Accession See DOI: 10.1039/x0xx00000x

Results and discussion

The initial bis(boramidinate)ferrocene FLP design was based on the reaction of 1,1'-dicarbodiimidoferrocenes with 9-BBN dimer. The reaction of 1 eq. of 1,1'-di-*t*-butylcarbodiimido ferrocene **1** with 1 eq. of 9-BBN dimer proceeds at 60 °C in benzene or toluene solution causing a darkening of the orange colored carbodiimide solution (Scheme 2). At room temperature the reactions are sluggish and significant amounts of the mono reduced carbodiimide can be observed by NMR. Capture of carbodiimides and boranes by boramidinates has been previously reported,[50] and shorter reaction times eliminate this problem resulting in a clean reaction and no appreciable intramolecular carbodiimide or additional 9-BBN capture. Boramidinate **2** is a liquid at room temperature which impeded the effective separation of traces of unreacted **1** and 9-BBN. Reaction of 1,1'-dimesitylcarbodiimide **3** with 9-BBN using similar conditions afforded boramidinate **4**, in this case upon cooling the product crystallized, allowing pure material to be isolated in 49% yield (Scheme 2).

Reduction of the carbodiimido substrates causes the appearance of a formamidinate signal in the ^{1}H NMR spectrum in C_6D_6 (**2**: δ 8.42 ppm, **4**: δ 8.83 ppm). The ^{11}B NMR is consistent with a tricoordinate boron center for both compounds (**2**: δ 53.5 ppm, **4**: δ 56.1 ppm). Interestingly, reduction of alkyl substituted **1** is favored through the N-ferrocene atom whereas for the aryl substituted analogue **3** reduction occurs through the N-mesityl atom even though it is more sterically shielded. The connectivity was established in solution by 2D NMR experiments and in the solid-state by XRD in the case of **4**.

Exposure of a degassed solution of the alkylboramidinate **2** in toluene to 1 atm of dry CO_2 gas leads to a yellow crystalline precipitate after standing overnight at room temperature. The crystals were identified as the symmetric CO_2 captured product **5** (Scheme 3) with a characteristic C=O FT-IR stretch observed at ν 1728 cm^{-1}. This compound is slightly soluble in dichloromethane and chloroform but decomposes in THF and DMSO. In solution a rearrangement occurs to give a mixture of both the symmetric **5** and the mono CO_2 captured product **6** (Scheme 3). We were able to stabilize **5** to obtain partial NMR characterization data under 6 atm of CO_2 but not long enough to obtain a reliable ^{11}B NMR signal that could be unambiguously assigned to **5** (SI Fig. S25). Capture of CO_2 induces a characteristic downfield shift of the formamidine hydrogen resonance to δ 8.89 ppm. In the solid-state under an inert atmosphere compound **5** is stable for weeks at room temperature. No decomposition of **5** occurred on exposure of the solid to a dynamic vacuum for 12 hours at room temperature.

When a degassed toluene solution of **2** was exposed to dry CO (1 atm) a semi-crystalline light-yellow solid precipitated within minutes. The crystals were identified as the symmetric CO captured product **7** (Scheme 3) with a characteristic C=O stretch at ν 1694 cm^{-1} in the FT-IR spectrum. We believe the precipitate might contain mono CO captured product, **8**, given the presence of a shoulder in the ν 1694 cm^{-1} peak. Compound **7** is insoluble in common aprotic NMR solvents. However, during NMR sample preparation we realized that there was a short induction period (aproximately 1 minute) before the compound completely dissolved in CD_2Cl_2. We believe this is caused by solvation triggered release of 1 equivalent of CO from **7** which gives rise to the more soluble mono CO captured product **8** (compound **2** is very soluble in chlorinated solvents). This was confirmed by the observation of **8** in the NMR spectrum (SI Fig. S26). Compound **7** is stable under 6 atm of CO for several days and this allowed us to obtain a reliable ^{11}B NMR spectrum (δ -3.4 ppm), consistent with the tetracoordinate carbamate bound boron atom (SI Fig. S28).

In contrast, exposure of a solution of arylboramidinate **4** to 1 atm of CO_2 or CO resulted in no visible precipitate formation.

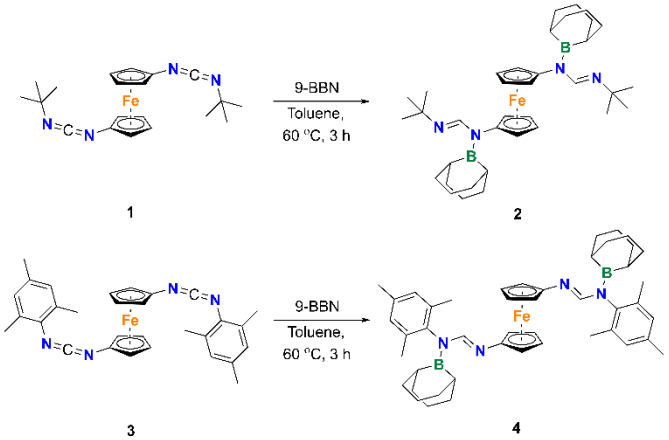

Scheme 2 Reduction of 1,1'-dicarbodiimidoferrocenes **1** and **3** with 9-BBN dimer to yield bis(boramidinate)ferrocenes **2** and **4**.

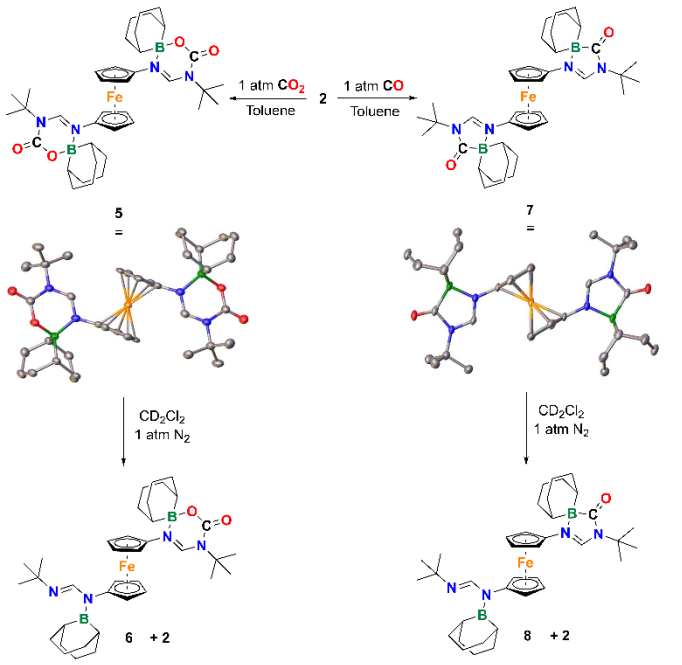

Scheme 3 Small molecule capture of *t*-butyl substituted boramidinate **2** with 1 atm of CO_2 or CO and subsequent release upon exposure to 1 atm of N_2.

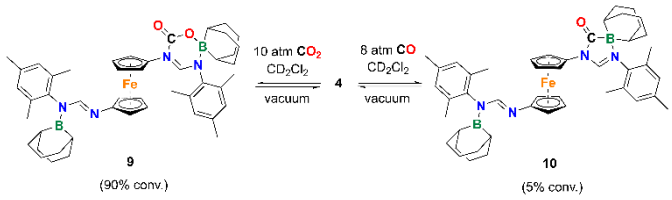

Scheme 4 Reactivity of mesityl substituted bis(boramidinate)ferrocene **4** towards elevated pressures of CO and CO_2.

The analysis of **4** in CD_2Cl_2 solution in a heavy walled NMR tube under CO_2 (1 atm) revealed the incipient formation of the mono CO_2 captured adduct **9** (Scheme 4). The appearance of two formamidine ^{1}H NMR peaks [δ 8.93 and δ 8.72 ppm] and the presence 4 triplets for the Cp-*H* resonances and 2 sets of singlets for the mesityl-$(CH_3)_2$ are consistent with the mono CO_2 captured product. A ^{13}C NMR *C*O_2 carbamate resonance is evident at δ 150.3 ppm which is correlated to the downfield formamidine hydrogen signal as proved by Heteronuclear Multiple Bond Correlation (HMBC). The ^{11}B NMR signals appear at δ 7.3 and δ 58.6 ppm. The analysis of the solution under elevated pressures of CO_2 showed increasing conversion to the mono captured adduct. At the highest pressure we could safely achieve using a thick-walled NMR tube (10 atm) the conversion is approximately 90% to the mono captured product based on the starting material (SI Fig. S29). The presence of the putative double CO_2 capture product cannot be unambiguously established due to peak overlap. The starting arylboraformamidinate **4** can be recovered cleanly by evaporating the solvent from the high-pressure NMR tube and subjecting the sample to ~12 h of dynamic vacuum. Exposure of **4** to increasing pressures of CO gas resulted in approximately 5% conversion to the mono CO capture product **10** at 8 atm of CO (Scheme 4). Likewise, **4** was regenerated after evaporation of the solvent and exposure to high vacuum.

We believe that steric bulk could have a significant role in the accessibility of the boron center of boramidates **2** and **4**. Inspection of the solid-state structure of the adamantyl substituted analogue of **2** shows that the boron atom is open for accommodating a Lewis acid (**2**$_{adamantyl}$, SI Fig. S1).[53] The boron atom in **4** is more shielded and the 9-BBN boracycle locked by the mesityl *ortho*-methyl substituents, an incoming small molecule would have to displace the mesityl substituent and interact with the boron atom.

The observation of a single quenched FLP in the bis(boramidinate)ferrocene scaffold was a promising step towards the isolation of an asymmetrically functionalized FLP. However, the highly reversible nature of the CO_2/CO binding, the need for elevated pressures to drive capture and the poor solubility of the adducts precluded the isolation and further characterization of the reactivity of the mono CO_2/CO captured products from the 9-BBN based system.

To overcome these problems, using a more electron deficient borane such as bis-pentafluorophenyl borane[54,55] seemed a reasonable alternative which should lead to a more robust tethered boramidinate FLP, which is less prone to reversible small molecule binding.[42,56] Reaction of 1,1'-di-*tert*-butylcarbodiimido ferrocene **1** with one equivalent of bis-pentafluorophenyl borane $[(C_6F_5)_2BH]_2$ in toluene yields crystalline bis(boramidinate) FLP **11** in good yield and excellent purity (Scheme 5). This molecule bears two boramidinate FLP moieties which appear to be equivalent in CD_2Cl_2, one formamidinate resonance by ^{1}H NMR at δ 7.93 ppm, a set of three well-defined resonances by ^{19}F NMR and an ^{11}B NMR shift consistent with tetracoordinated boron in solution [δ 2.21 ppm]. Despite the relatively large size of the pentafluorophenyl substituted boramidinates the rotation through the ferrocene axis is not hindered, at least in solution at room temperature. The NMR assignment was consistent with the solid-state structure of a four-membered cyclic boramidinate (SI Fig. S3).

Our attempts to crystallize **11** lead to the XRD characterization of side product **12** (Scheme 5) where one of the FLPs has incorporated an additional $(C_6F_5)_2BH$ to relieve the strained four membered ring to form a six membered borane bridged heterocycle (SI Table S2). We decided to pursue this synthetic route and reacted **11** with two equivalents of $[(C_6F_5)_2BH]_2$ to obtain the boramidinate adduct **13** (Scheme 6). The structural parameters of the heterocycle in **13** are comparable to those observed in **12**. Compound **13** is sufficiently soluble in CD_2Cl_2 to obtain spectroscopic data although it is sparingly soluble in common solvents which precluded us from pursuing further chemistry. Binding of the $HB(C_6F_5)_2$ fragment causes a downfield shift in the ^{1}H NMR formamidine resonance to δ 9.03 ppm. The formamidine and N-$C(CH_3)_3$ hydrogens appear to be equivalent at room temperature, but the Cp-*H* hydrogens of ferrocene appear as a broad signal. The ^{1}H NMR resonance for the B-*H*-B hydrogen arises at δ 2.72 ppm. The steric bulk introduced by the additional pentafluorophenyl rings likely hinders the free rotation through the ferrocene tether (SI Fig. S39). The ^{11}B NMR signal, although weak even in a concentrated sample, is observed at δ 12.44 ppm.

At this point we realized that both boramidinate arms in **11** did not engage in cooperative FLP chemistry and that by careful synthetic control we might be able to sequentially control the reactivity of both FLP moieties. We first focused on the synthesis of symmetric small molecule adducts. The CO adduct **14** was prepared by exposing a CD_2Cl_2 solution of **11** to CO (1 atm) (Scheme 6). The reaction occurs in seconds as judged by the rapid darkening of the solution from orange to dark red. Capture of CO causes a general downfield shift in the ^{1}H NMR spectrum and the ^{11}B NMR signal shifts upfield to δ -11.02 ppm.

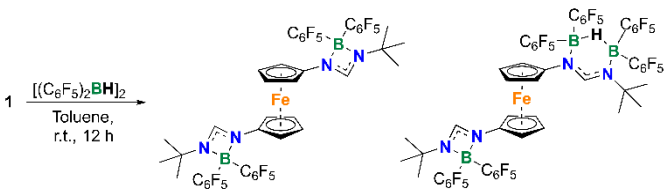

Scheme 5 Reduction of 1,1'-di-*t*-butyl-carbodiimidoferrocene **1** with Piers' borane to yield bis(boramidinate)ferrocene **11** and traces of **12**.

ARTICLE

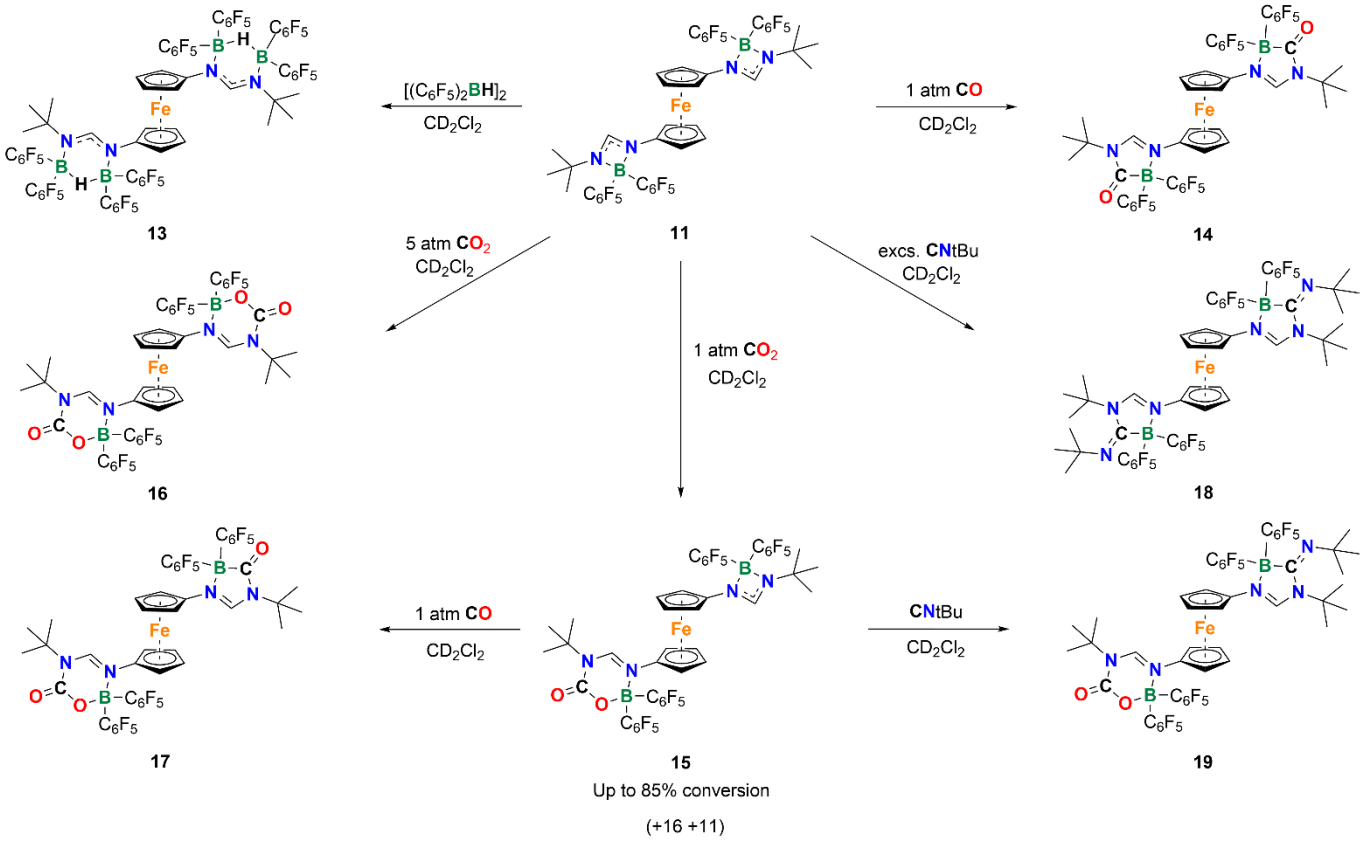

Scheme 6 Reactivity of boramidinate **11** towards $[(C_6F_5)_2BH]_2$, CO, CO_2 and CNtBu.

Observation of the ^{13}C NMR *CO* signal required the use of isotopically enriched ^{13}CO with a broad signal centered at δ 197.5 ppm. Additionally, incorporation of CO was confirmed by FT-IR revealing the C=O stretching band at ν 1745 cm^{-1}.

Next, we set out to isolate the symmetric CO_2 adduct **16** (Scheme 6). Exposure of a CD_2Cl_2 solution of **11** to CO_2 (1 atm) for 24 hours resulted in a sluggish reaction giving rise to a complex reaction mixture containing unreacted **11**, monofunctionalized boramidinate **15** and traces of the symmetrically functionalized product **16** (Scheme 6). Full conversion to **16**, on a reasonable timescale, required to use 5 atm of CO_2 for 2 weeks. Likewise, a general downfield shift of the formamidine hydrogen was observed upon CO_2 binding and the ^{11}B NMR signal shifts to δ 0.25 ppm. The ^{13}C NMR *CO*$_2$ carbamate signal is observed at δ 145.8 ppm. The corresponding FT-IR C=O stretching appears at ν 1759 cm^{-1}.

Although we have not been able to isolate an analytically pure sample of the monofunctionalized **15** without traces of **11** or **16** being present, the observation that it is stable in degassed solutions by freeze-pump-thaw cycles**,** gave us the opportunity to characterize it *in-situ*. The NMR characterization data in CD_2Cl_2 confirms the asymmetric boramidinate-CO_2 adduct composition for **15** with 4 Cp-*H* characteristic triplet resonances in the ^1H NMR spectrum. Both arms have well defined formamidine hydrogen signals arising at δ 9.05 ppm and δ 8.00 ppm. The carbamate *CO*$_2$ ^{13}C NMR signal appears at δ 146.1 ppm. Desymmetrization of the boramidinate arms also causes the appearance of two sets of ^{19}F NMR signals. By carefully controlling the conversion we have been able to identify two independent ^{11}B NMR signals arising at δ 0.22 and δ 2.26 ppm comparable with the shifts of **11** and the symmetric CO_2 adduct **16**. Our attempts to crystallize **15** have only yielded thin, brittle, crystalline plates identified in the solid-state by single crystal XRD studies to contain a mixture of $[(C_6F_5)_2BH]_2$ borane, **13** and the CO_2 adduct **16**.

The CO_2 molecule is a very poor ligand compared to CO and this is consistent with the slower rates observed in the reaction with boramidinate **11**. The first CO_2 capture occurs significantly faster than the second capture allowing for the introduction of a more reactive species (CO) that would preferentially react over CO_2 in the second step giving rise to an asymmetrically functionalized FLP. To test our hypothesis a valved NMR tube containing **11** under 1 atm of CO_2 was reacted until conversion to **15** reached ~60%. Degassing the CO_2 and refilling the tube immediately with 1 atm of CO yields the asymmetrically functionalized FLP **17** (Scheme 6) along with **14** and **16**.

Producing an analytically pure sample of **17** proved challenging. The maximum yield of **17** (quantified by NMR) so far achieved is approximately 85%. Extending the reaction time to maximize the conversion to **15** results in buildup of **16** in the solution. Under these conditions purification by recrystallization consistently resulted in enrichment of the sample in component **16**.

Analogous to **15**, the $^{1}H/^{13}C$ NMR spectra of **17** are indicative of an asymmetrically substituted compound. The ^{1}H NMR spectrum shows two resonances for the formamidine hydrogens at δ 8.92 and δ 8.72 ppm, 4 triplets for the ferrocene Cp-*H*s and two N-C(CH_3)$_3$ singlets. The connectivity was confirmed by 2D NMR techniques. The ^{13}C NMR CO_2 adduct signal arises at δ 145.8 ppm. Additionally, the formate adduct of the molecular ion has been observed by HRMS-ESI further supporting our structural assignment (SI Fig. S81).

Attempts to crystallize the asymmetric species for XRD also proved difficult because traces **14** and **16** act as templating agents for the crystallization of **17**. Crystallization experiments from solutions containing **16** as impurity produced crystals of **17** crystallizing in the *Cc* space group. Analysis of the solid-state structure shows substitutional disorder between the asymmetric arms. Samples containing impurities of **14** crystallize with **17** in the $P2_1/n$ space group, in this symmetry arrangement both arms are well defined supporting the connectivity assignment of **17** (Figure 1). In both cases extensive single crystal screening was required to obtain single crystals of **17** since the majority of the crystallized samples were composed of crystals of **14** or **16**.

To circumvent the purification difficulties arising from the similar sizes of CO and CO_2 we decided to exchange CO with the much larger *tert*-butyl isocyanide (CNtBu), a widespread CO surrogate[57,58] and already known to react with boramidinates in a similar fashion to CO.[42] Again, we first synthetized the symmetrically CNtBu functionalized FLP **18** using an excess of CNtBu to confirm a fast reaction analogous to CO (Scheme 6). In this case the addition of CNtBu results in a color change of the CD_2Cl_2 solution of **11** from orange to yellow with a concomitant shift of the formamidine ^{1}H NMR signal to δ 8.52 ppm. The ^{11}B NMR signal was observed at δ -9.82 ppm.

Treatment of a dichloromethane solution containing approximately 65% of compound **15** with excess CNtBu resulted in an immediate color change from dark to light orange forming the asymmetrically functionalized FLP **19** (Scheme 6) and the soluble symmetric CNtBu adduct **18** which could be more easily purified by washing the crude reaction with chloroform. The FT-IR C=O stretch of **19** arises at ν 1751 cm^{-1}. The formamidinate ^{1}H NMR signals in **19** appear close to their symmetrical counterparts **16** and **18** respectively [δ 8.95 and δ 8.50 ppm] but do not overlap. The ^{11}B NMR spectrum shows two resonances at δ 0.22 and δ -9.81 ppm which closely match the shift of the symmetrical counterparts (Figure 2). The ^{19}F NMR spectrum shows the characteristic pattern of the asymmetrical arrangement with two sets of 3 signals again resembling the shifts of the symmetric **16** and **18** counterparts.

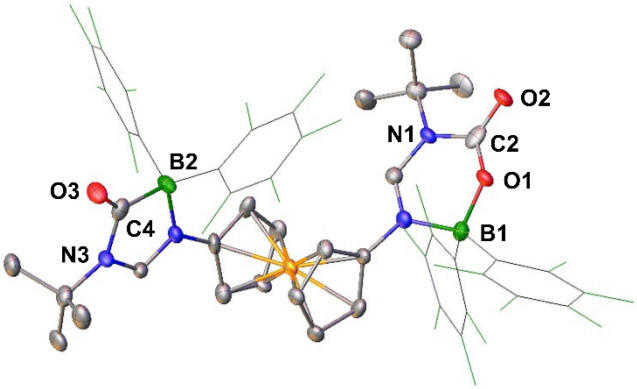

Figure 1 Solid-state structure of **17** where the CO and CO_2 boramidinate adducts are well defined. Selected bond lengths (Å): B1-O1 1.512(15), C2-N1 1.437(15), C2-O1 1.292(12), C2-O2 1.233(16), B2-C4 1.645(16), C4-N3 1.436(15), C4-O3 1.228(13). Ellipsoids set at 50% probability, pentafluorophenyl groups are depicted as wireframe and hydrogens have been removed for clarity.

In the final part of our study, we turned our attention to characterize the electrochemical properties of these ferrocene bearing molecules by cyclic voltammetry (CV). There has been recent interest in the electrochemistry of disubstituted ferrocenes.[59] However, to the best of our knowledge there has been no previous electrochemical study of boramidinate based FLPs and their small molecule adducts. In our work we focused on the more chemically stable symmetric derivatives of **11**.

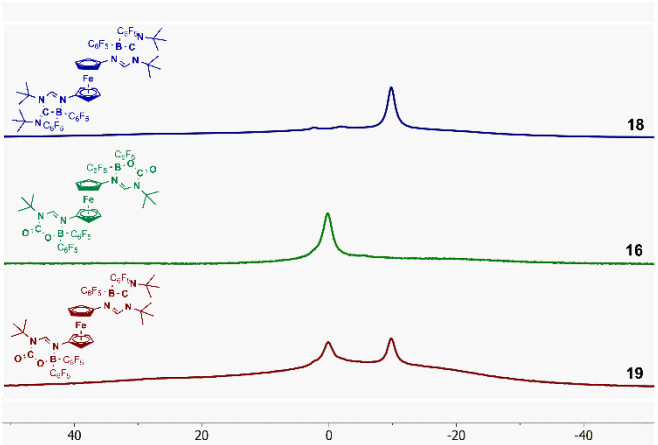

Figure 2 Stacked ^{11}B NMR spectra of **18**, **16** and **19** in CD_2Cl_2. The two resonances of boramidinate **19** resemble the features arising in the spectrum the symmetric adduct counterparts **18** and **16.**

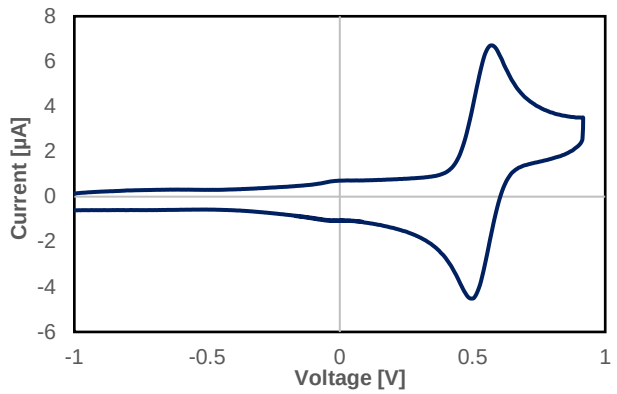

Figure 3 Cyclic voltammogram of symmetric CO_2 adduct **16** (1 mM) in 0.1 M $[NBu_4][PF_6]$ dichloromethane solution.

The CV of boramidinate **11** shows a reversible wave at $E_{1/2}$ = 50 mV assigned to the $[Fc^0/Fc^+]$ couple. Analysis of the scan rate dependence revealed a freely diffusing redox event (SI Fig. S4). Scanning at higher potentials shows an irreversible oxidation event (880 mV) leading to chemical decomposition likely involving the four-membered boramidinate heterocycle. Repeated scanning of **11** results in decomposition. The symmetric CO adduct **14** shows a freely diffusing quasi-reversible $[Fc^0/Fc^+]$ wave shifted to more oxidizing potential [$E_{1/2}$ = 410 mV] (SI Fig. S10). The CO_2 adduct **16** (Figure 3) has freely diffusing reversible wave at $E_{1/2}$ = 535 mV. In these two cases no other event is observed at more oxidizing potentials due to the higher stability of the small molecule quenched FLP. Despite its poor solubility we have also been able to acquire the voltammogram of **13**, which shows a quasi-reversible wave with $E_{1/2}$ = 550 mV (SI Fig. S7). Lastly, compound **18** decomposes irreversibly in the electrochemical cell likely through oxidation of the C=NtBu bond (SI Fig. S16).

Experimental

Operations were performed using standard Schlenk techniques or in a VAC HE-63P nitrogen filled glovebox. Dry deoxygenated solvents were obtained from an Innovative Technology Pure Solve MD solvent purification system and stored over activated 4 Å molecular sieves. Deuterated solvents were degassed by the freeze-pump-thaw method (CD_2Cl_2, $CDCl_3$) or distilled from sodium/benzophenone ketyl (C_6D_6, C_7D_8) and stored over activated 4 Å molecular sieves in Teflon valved flasks. Piers' Borane, 1,1'-diterbutylcarbodiimidoferrocene **1** and 1,1'-dimesitylcarbodiimidoferrocene **3** were prepared according to published procedures.[26,40,60] 9-boracyclo[3.3.1]nonane dimer was purchased from Alfa Aesar and recrystallized from dimethoxyethane as previously reported.[61]

Compound 2 [$C_{36}H_{56}N_4B_2Fe$] Equimolar amounts of 1,1'-di-*tert*-butylcarbodiimidoferrocene **1** (100 mg, 0.26 mmol) and 9-boracyclo[3.3.1]nonane dimer (65 mg, 0.26 mmol) in toluene (1.5 mL) were heated at 60 °C for 3 hours. The solvent was removed under vacuum to afford compound **2** quantitatively as an orange oil. **^{1}H-NMR** (400 MHz, Benzene-d_6) δ 8.42 (s, 2H, N-C(*H*)=N), 4.38 (t, *J* = 1.9 Hz, 2H, Cp-*H*), 4.08 (t, *J* = 1.9 Hz, 2H, Cp-*H*), 1.95-1.88 (m, 28H, -CH_2- + -C*H*-), 1.29 (s, 18H, -C(CH_3)$_3$)). **^{13}C-NMR** (100 MHz, Benzene-d_6) δ 150.3 (N-*C*(H)=N), 102.0 (Cp-*C*-N), 66.6 (Cp-*C*H), 66.5 (Cp-*C*H), 55.1 (-*C*(CH$_3$)$_3$), 33.7 (-CH_2-), 30.7 (-C(*C*H$_3$)$_3$), 25.9 (br, -*C*H-), 23.7 (-CH_2-). **^{11}B-NMR** (192 MHz, Benzene-d_6) δ 53.5. **Melting Point**: liquid at room temperature.

Compound 4 [$C_{46}H_{60}N_4B_2Fe$] 1,1'-dimesitylcarbodiimidoferrocene **3** (100 mg, 0.20 mmol) and 9-boracyclo[3.3.1]nonane dimer (49 mg, 0.20 mmol) were dissolved in C_6D_6 (0.5 mL), placed in a resealable ampoule and heated at 60° C for 3 hours. Cooling to room temperature afforded an orange crystalline solid which was filtered, washed with hexane (3 x 0.5 mL) and dried under vacuum to afford the title compound. Yield (73 mg, 49%). **^{1}H-NMR** (400 MHz, Methylene Chloride-d_2) δ 8.75 (s, 2H, N-C(*H*)=N), 6.94 (s, 4H, Aryl-*H*), 4.19 (t, *J* = 1.9 Hz, 4H, Cp-*H*), 3.98 (t, *J* = 1.9 Hz, 4H, Cp-*H*), 2.32 (s, 6H, Aryl-CH_3), 2.10 (s, 12H, Aryl-CH_3), 2.05 – 1.85 (m, 14H), 1.74 – 1.56 (m, 8H), 1.49 – 1.35 (m, 4H), 0.69 (br, 2H). **^{13}C-NMR** (101 MHz, Methylene Chloride-d_2) δ 152.4 (N-*C*(H)=N), 138.7 (C_q), 136.2 (C_q), 134.6 (C_q), 129.2 (Aryl-*C*H), 67.8 (Cp-*C*H), 63.1 (Cp-*C*H), 33. 9 (-CH_2-), 33.7 (-CH_2-), 25.3 (BBN-*C*H), 24.7 (-*C*H-), 23.5 (-CH_2-), 21.1 (Aryl-*C*H$_3$), 18.5 (Aryl-*C*H$_3$). **^{11}B NMR** (192 MHz, Benzene-d_6) δ 57.1. **FT-IR** (ATR, cm^{-1}) 3083, 2981, 2908, 2882, 2835, 1632, 1483, 1469, 1445, 1403, 1375, 1358, 1330, 1308, 1284, 1271, 1224, 1191, 1139, 1099, 1039, 1019, 962, 936, 908, 848, 838, 821, 808, 745, 698, 680, 655, 626, 615, 580, 572, 557, 538, 513, 493, 474, 463, 434, 408. **Elemental Analysis** Experimental C, 73.92; H, 7.92; N 7.30. Calc. for [$C_{46}H_{60}B_2FeN_4$]: C, 74.01; H, 8.10; N, 7.51. **Melting Point**: 246-247 °C.

Preparation of compound 5 [$C_{38}H_{56}N_4B_2O_4Fe$] Equimolar amounts of 1,1'-di-*tert*-butylcarbodiimidoferrocene **2** (100 mg, 0.26 mmol) and 9-boracyclo[3.3.1]nonane dimer (65 mg, 0.26 mmol) in toluene (1.5 mL) were heated at 60 °C for 3 hours. The solution was subjected to 3 freeze-pump-thaw cycles and refilled with 1 atm of CO_2. Warming to room temperature and standing overnight produces a light-yellow crystalline precipitate, the supernatant was removed, and the crystals were washed with toluene (1 mL) and pentane (3 x 1 mL) and dried under vacuum for 1 h. Yield of crystalline yellow solid (84 mg, 48%). **^{1}H-NMR** (500 MHz, Methylene Chloride-d_2) δ 8.89 (s, 2H, N-C(*H*)=N), 4.49 (t, *J* = 1.9 Hz, 4H, Cp-*H*), 4.39 (t, *J* = 1.9 Hz, 4H, Cp-*H*) 1.93-1.90 (m, -CH_2-), 1.77-1.70 (m, , -CH_2-) 1.67 (-C(CH_3)$_3$), 1.51-1.41 (m, , -CH_2-), 1.15-1.12 (m, -CH_2-), 0.67 (br, 4H, -C*H*-). **^{13}C-NMR** (126 MHz, Methylene Chloride-d_2) partial, δ 159.2 (N-*C*(H)=N), 150.0 (N-(*CO*)-O-B), 106.8 (Cp-*C*-N), 69.2 (Cp-*C*H), 67.8 (Cp-*C*H), 60.6 (-*C*(CH$_3$)$_3$), 32.1 (-CH_2-), 31.1 (-CH_2-), 29.7 (-C(CH_3)$_3$), 24.6 (-CH_2-), 24.3 (-CH_2-). **FT-IR** (ATR, cm^{-1}) 3117, 2978, 2953, 2912, 2853, 2827, 2126, 1728, 1625, 1484, 1449, 1389, 1371, 1321, 1279, 1236, 1193, 1124, 1091, 1064, 1041, 1029, 974, 964, 935, 912, 870, 847, 815, 789, 728, 693, 530, 464, 438. **Melting Point**: 131-133 °C (gas evolution).

Compound 7 [$C_{38}H_{56}N_4B_2O_2Fe$] Equimolar amounts of 1,1'-di-*tert*-butylcarbodiimidoferrocene **2** (100 mg, 0.26 mmol) and 9-boracyclo[3.3.1]nonane dimer (65 mg, 0.26 mmol) in toluene (1.5 mL) were heated at 60 °C for 3 hours. The resulting solution was subjected to a freeze-pump-thaw cycle and the flask carefully refilled with 1 atm of CO. Precipitation of the title compound occurs immediately and is completed in <5 minutes. The supernatant was removed, and the crystalline residue was washed with toluene (2 x 1 mL), pentane (2 x 2 mL) and dried under vacuum for 10 minutes. Yield of yellow microcrystalline solid (104 mg, 53%). **^{1}H-NMR** (500 MHz, Methylene Chloride-d_2), partial, δ 9.15 (s, 2H, N-C(*H*)=N), 4.42 (t, *J* = 2.0 Hz, 2H, Cp-*H*), 4.39 (t, *J* = 1.9 Hz, 2H, Cp-*H*), 2.18 (m, 4H, -CH_2-), 1.57 (s, 18H, -C(C*H*$_3$)$_3$)), 0.64 (br, 4H, -C*H*-). **^{13}C-NMR** (126 MHz, Methylene Chloride-d_2), partial, δ 161.6 (N-*C*(H)=N), 106.7 (Cp-*C*-N), 70.3 (Cp-*C*H), 67.3 (Cp-*C*H), 56.0 (-*C*(CH$_3$)$_3$), 31.0 (-*C*H$_2$-), 30.6 (-*C*H$_2$-), 29.0 (-C(*C*H$_3$)$_3$), 24.8 (-*C*H$_2$-) 24.4 (-*C*H$_2$-), 23.7 (-*C*H-). **^{11}B-NMR** (148 MHz, Methylene Chloride-d_2) δ -3.4. **FT-IR** (ATR, cm^{-1}) 2974, 2934, 2839, 1694, 1644, 1599, 1483, 1447, 1407, 1365, 1280, 1221, 1201, 1110, 1029, 959, 937, 904, 830, 791, 764, 727, 705, 694, 674, 566, 539, 525, 492, 462, 442, 417. **Melting Point**: 103 °C (gas evolution).

Compound 6 [$C_{47}H_{60}N_4B_2O_2Fe$] *Only NMR characterization data at 10 atm of CO_2 is reported for compound **6**.* **^{1}H-NMR** (500 MHz, Methylene Chloride-d_2) partial, δ 8.93 (s, 1H, N-C(*H*)=N), 8.72 (s, 1H, N-C(*H*)=N), 7.03 (s, 2H, Aryl-H), 6.94 (s, 2H, Aryl-H), 4.34 (t, *J* = 1.9 Hz, 2H, Cp-*H*), 4.25 (t, *J* = 1.9 Hz, 2H, Cp-*H*), 4.18 (t, *J* = 1.9 Hz, 2H, Cp-*H*), 3.97 (t, *J* = 1.9 Hz, 2H, Cp-*H*), 2.34 (s, 3H, Aryl-C*H*$_3$), 2.31 (s, 3H, Aryl-C*H*$_3$), 2.26 (s, 6H, Aryl-C*H*$_3$), 2.11 (s, 6H, Aryl-C*H*$_3$). **^{13}C-NMR** (126 MHz, Methylene Chloride-d_2) partial, δ 161.3 (N-*C*(H)=N), 153.4 (N-*C*(H)=N), 150.3 (N-(*C*O)-O-B), 140.4 (C$_q$), 138.5 (C$_q$), 136.7 (C$_q$), 136.3 (C$_q$), 134.6 (C$_q$), 134.2 (C$_q$), 130.4 (Aryl-*C*H), 129.4 (Aryl-*C*H), 108.9 (Cp-*C*-N), 106.6 (Cp-*C*-N), 69.4 (Cp-*C*H), 68.7 (Cp-*C*H), 67.3 (Cp-*C*H), 63.7 (Cp-*C*H), 21.2 (Aryl-*C*H$_3$), 21.1 (Aryl-*C*H$_3$), 18.6 (Aryl-*C*H$_3$), 18.5 (Aryl-*C*H$_3$). **^{11}B-NMR** (148 MHz, Methylene Chloride-d_2) δ 58.6, 7.30.

Compound 8 [$C_{47}H_{60}N_4B_2OFe$] *Only ^{1}H-NMR characterization data at 8 atm of CO is reported for compound **8**.* **^{1}H-NMR** (500 MHz, Methylene Chloride-d_2), partial δ 9.09 (s, 1H, N-C(*H*)=N), 4.33 (t, *J* = 2.0 Hz, 2H, Cp-*H*), 4.28 (t, *J* = 1.9 Hz, 2H, Cp-*H*), 4.10 (t, *J* = 1.9 Hz, 2H, Cp-*H*), 4.03 (t, *J* = 1.6 Hz, 2H, Cp-*H*).

Compound 11 [$C_{44}H_{28}N_4B_2F_{20}Fe$] In a vial 1,1'-di-*tert*-butylcarbodiimidoferrocene **1** (120 mg, 0.33 mmol) and Piers' borane [BH(C$_6$F$_5$)$_2$]$_2$ (219 mg, 0.33 mmol,) were combined in toluene (1.5 mL) giving rise to a red solution. This solution was layered with hexane (10 mL). Standing overnight crystals developed. The supernatant liquid was removed, and the crystals were washed with pentane (1 mL) affording the title compound as a red crystalline material. Yield (192 mg, 57%). **^{1}H-NMR** (500 MHz, Methylene Chloride-d_2) δ 7.93 (s, 2H, N-C(*H*)=N), 3.91 (t, *J* = 1.9 Hz, 4H, Cp-*H*), 3.62 (t, *J* = 1.9 Hz, 4H, Cp-*H*), 1.22 (s, 18H, -C(C*H*$_3$)$_3$)). **^{13}C-NMR** (126 MHz, Methylene Chloride-d_2) δ 158.0 (N-*C*(H)=N), 149.3 (m, Aryl-*C*-F), 147.4 (m, Aryl-*C*-F), 141.9 (m, Aryl-*C*-F), 139.9 (m, Aryl-*C*-F), 138.7 (m, Aryl-*C*-F), 136.8 (m, Aryl-*C*-F), 97.2 (Cp-*C*-N), 66.9 (Cp-*C*H), 60.0 (Cp-*C*H), 54.4 (-*C*(CH$_3$)$_3$), 29.7 (-C(*C*H$_3$)$_3$). **^{19}F-NMR** (376 MHz, Methylene Chloride-d_2) δ -133.0 (dd, *J* = 23.8, 8.9 Hz, o-*F*), -155.5 (t, *J* = 20.3 Hz, p-*F*), -163.5 (td, *J* = 22.5, 8.9 Hz, m-*F*). **^{11}B-NMR** (128 MHz, Methylene Chloride-d_2) δ 2.37. FT-IR (ATR, cm^{-1}) 2982, 1647, 1566, 1542, 1520, 1456, 1388, 1373, 1290, 1228, 1211, 1180, 1101, 1020, 981, 957, 837, 825, 801, 768, 752, 742, 691, 655, 628, 579, 555, 507, 486, 432, 406. **HRMS** (ESI): m/z calcd. $C_{44}H_{31}B_2F_{20}FeN_4O^+$: 1089.1724 [M+H$_2$O+H]$^+$; found: 1089.1723 m/z [$C_{44}H_{31}B_2F_{20}FeN_4O^+$]. **Elemental Analysis** Experimental C, 49.38; H, 2.70; N, 5.12. Calc. for [$C_{44}H_{28}N_4B_2F_{20}Fe$]: C, 49.38; H, 2.64; N, 5.24. **Melting Point** 172-175 °C.

Compound 13 [$C_{68}H_{30}N_4B_4F_{40}Fe$] Boramidinate **11** (10 mg, 9.3 mmol) was dissolved in dichloromethane (1 mL), solid Piers' borane was added (6.5 mg, 9.3 mmol). The solution turns from orange to yellow as Piers' borane dissolves and reacts, and after approximately 15 minutes is followed by precipitation of the title compound. The supernatant was removed, and the remaining light-yellow colored powder was washed with dichloromethane (1 mL), pentane (1 mL) and dried to obtain compound **13**. Yield (15 mg, 92%). **^{1}H-NMR** (500 MHz, Methylene Chloride-d_2) δ 9.03 (s, 2H, N-C(*H*)=N), 4.41 (br, Cp-*H*, 8H), 2.72 (br, B-*H*-B), 1.42 (s, 18H, -C(C*H*$_3$)$_3$). ^{13}C-NMR (126 MHz, Methylene Chloride-d_2) δ partial 167.7 (N-*C*(H)=N), 103.9 (Cp-*C*-N), 69.7 (Cp-*C*H), 67.7 (Cp-*C*H), 61.3 (-*C*(CH$_3$)$_3$), 30.8 (-C(*C*H$_3$)$_3$). **^{19}F-NMR** (376 MHz, Methylene Chloride-d_2) δ -129.4 (br, o-*F*), -155.6 (br, p-*F*), -153.8 (br, p-*F*), -162.9 (br, m-*F*). **^{11}B-NMR** (128 MHz, Methylene Chloride-d_2) δ 12.44. FT-IR (ATR, cm^{-1}) 1790 (br), 1647, 1596, 1521, 1464, 1415, 1374, 1346, 1294, 1265, 1176, 1120, 1098, 1038, 983, 965, 907, 876, 848, 831, 798, 773, 753, 740, 711, 689, 682, 664, 641, 623, 579, 559, 541, 511, 457, 441. **HRMS** (ESI): Inconclusive: unidentifiable fragments, molecular ion not observed. **Melting Point** 167 °C (decomposition).

Compound 14 [$C_{46}H_{28}N_4B_2F_{20}O_2Fe$] Compound **11** (45 mg, 0.042 mmol) in CD_2Cl_2 (1.5 mL) was placed in a valved NMR tube, degassed by the freeze-pump-thaw method, refilled with 1 atm of CO and shaken. The reaction is complete in less than 1 min. This solution was transferred to a vial and layered with hexane (1.5 mL) to afford orange fine needles of the title compound after 1 day. The supernatant was removed, the residue washed with pentane (1 mL) and dried under vacuum to obtain compound **14**. Yield (30 mg, 63%). **^{1}H-NMR** (500 MHz, Methylene Chloride-d_2) δ 8.68 (s, 2H, N-C(*H*)=N), 4.19 (t, *J* = 2.0 Hz, 4H, Cp-*H*), 3.83 (t, *J* = 2.0 Hz, 4H, Cp-*H*), 1.58 (s, 18H, -C(C*H*$_3$)$_3$). **^{13}C-NMR** (126 MHz, Methylene Chloride-d_2), partial, δ 197.5 (br, *C*=O), 158.9 (N-*C*(H)=N), 99.0 (Cp-*C*-N), 69.2 (Cp-*C*H), 63.1 (Cp-*C*H), 58.1 (-*C*(CH$_3$)$_3$), 28.5 (-C(*C*H$_3$)$_3$). **^{19}F-NMR** (376 MHz, Methylene Chloride-d_2) δ -131.2 (dd, *J* = 23.5, 8.6 Hz, o-*F*), -155.6 (t, *J* = 20.3 Hz, p-*F*), -162.4 (ddd, *J* = 23.7, 20.0, 8.7 Hz, m-*F*). **^{11}B-NMR** (128 MHz, Methylene Chloride-d_2) δ -11.0. FT-IR (ATR, cm^{-1}) 2983, 1745, 1645, 1594, 1517, 1474, 1458, 1433, 1374, 1355, 1237, 1219, 1201, 1121, 1104, 1051, 1037, 1010, 971, 935, 898, 854, 837, 815, 787, 772, 757, 748, 713, 649, 632, 615, 578, 569, 501, 490, 463, 422. **HRMS** (ESI): m/z calcd. $C_{47}H_{29}B_2F_{20}FeN_4O_4^-$: 1171.1427 [M+HCOO]$^-$; found: 1171.1389. **Elemental Analysis** Experimental C, 48.83; H,

2.47; N, 4.93. Calc. for [$C_{46}H_{28}B_2F_{20}FeN_4O_2$]: C, 49.06; H, 2.51; N, 4.98. **Melting Point**: 189-190 °C (gas evolution).

Compound 16 [$C_{46}H_{28}N_4B_2F_{20}O_4Fe$] Compound **11** (40 mg, 37 mmol) was dissolved in CD_2Cl_2 (1 mL) and placed in a high-pressure NMR tube. The solution was subjected to 3 freeze-pump-thaw cycles, refilled with 5 atm of CO_2 and secured in a rocking platform. As judged by NMR the reaction reaches completion in 2 weeks. The resulting suspension was placed in a vial, the tubed washed with dichloromethane (3 x 1 mL) and the extracts combined to give a light orange solution which was layered with pentane (10 mL). After one day the supernatant was removed, the crystalline residue washed with pentane (1 mL) and dried under vacuum to obtain the title compound as a light yellow crystalline solid. Yield (17 mg, 40%). **^{1}H-NMR** (500 MHz, Methylene Chloride-d_2) δ 8.91 (s, 2H, N-C(*H*)=N), 4.32 (t, *J* = 2.0 Hz, 4H, Cp-*H*), 4.20 (t, *J* = 2.0 Hz, 4H, Cp-*H*), 1.63 (s, 18H, -C(CH_3)$_3$). ^{13}C-NMR (126 MHz, Methylene Chloride-d_2), partial, δ 157.1 (N-*C*(H)=N), 149.4 (br, Aryl-*C*-F), 147.5 (br, Aryl-*C*-F), 145.8 (N-(*C*O)-O-B), 142.2 (br, Aryl-*C*-F), 140.2 (br, Aryl-*C*-F), 138.6 (br, Aryl-*C*-F), 136.6 (br, Aryl-*C*-F), 102.8 (Cp-*C*-N), 69.2 (Cp-*C*H), 67.3 (Cp-*C*H), 63.1 (-*C*(CH$_3$)$_3$), 29.5 (-C(*C*H$_3$)$_3$). **^{19}F-NMR** (376 MHz, Methylene Chloride-d_2) δ -134.2 (dd, *J* = 23.5, 9.2 Hz, o-*F*), -154.5 (t, *J* = 20.1 Hz, p-*F*), -162.2 (ddd, *J* = 23.6, 20.0, 9.1 Hz, m-*F*). **^{11}B-NMR** (128 MHz, Methylene Chloride-d_2) δ 0.25. FT-IR (ATR, cm^{-1}) 1759, 1644, 1519, 1462, 1375, 1330, 1290, 1276, 1227, 1185, 1100, 1035, 975, 937, 925, 862, 832, 816, 794, 770, 754, 740, 732, 702, 690, 672, 644, 578, 560, 513, 487. **HRMS** (ESI): m/z calcd. $C_{46}H_{32}B_2F_{20}FeN_5O_4^+$ 1176.1681 [M+NH$_4$]$^+$; found: 1176.1713. **Melting Point**: 149-150 °C (gas evolution).

Compound 15 [$C_{45}H_{28}N_4B_2F_{20}O_2Fe$] A typical procedure for the generation of compound **15** in CD_2Cl_2 is described here. Boramidinate **11** (40 mg, 0.037 mmol) was dissolved in CD_2Cl_2 (1 mL) and placed in a valved NMR tube. The solution was freeze-pump-thawed 3 times and refilled with 1 atm of CO_2. The tube was placed in a rocking platform for 40 hours and conversion followed by NMR. Composition of the crude mixture after 40 h (**11**: 14%, **15**: 75%, **16**: 11%). **^{1}H-NMR** (500 MHz, Methylene Chloride-d_2) δ 9.05 (s, 1H, N-C(*H*)=N), 8.00 (s, 1H, N-C(*H*)=N), 4.20 (t, *J* = 2.0 Hz, 2H, Cp-*H*), 4.10 (t, *J* = 2.0 Hz, 2H, Cp-*H*), 3.90 (t, *J* = 2.0 Hz, 2H, Cp-*H*), 3.70 (t, *J* = 2.0 Hz, 2H, Cp-C*H*), 1.64 (s, 9H, (-CCH_3)$_3$), 1.23 (s, 9H, -C(CH_3)$_3$). **^{13}C-NMR** (126 MHz, Methylene Chloride-d_2), partial, δ 158.0 (N-*C*(H)=N), 156.9 (N-*C*(H)=N), 146.1 (N-(*C*O)-O-B), 102.0 (Cp-*C*-N), 99.0 (Cp-*C*-N), 69.0 (Cp-*C*H), 66.8 (Cp-*C*H), 66.8 (Cp-*C*H), 62.6 (-*C*(CH$_3$)$_3$), (59.8 (Cp-*C*H), 54.9 (-*C*(CH$_3$)$_3$), 29.6 (-C(*C*H$_3$)$_3$), 29.5 (-C(*C*H$_3$)$_3$). **^{19}F-NMR** (376 MHz, Methylene Chloride-d_2), partial, δ -131.1 (dd, *J* = 23.0, 9.1 Hz, o-*F*), -134.5 (dd, *J* = 23.4, 9.1 Hz, o-*F*), -154.8 (t, *J* = 20.3 Hz, p-*F*), -155.1 (t, *J* = 20.2 Hz, p-*F*), -162.7 ((ddd, *J* = 23.5, 20.5, 9.3 Hz, m-*F*). **^{11}B-NMR** (160 MHz, Methylene Chloride-d_2) δ 0.22, 2.26. **HRMS** (ESI): m/z calcd. $C_{45}H_{29}B_2F_{20}FeN_4O_2Na^+$ 1137.1336 [M+Na]$^+$; found: 1137.1354.

Compound 17 [$C_{46}H_{28}N_4B_2F_{20}O_3Fe$] *The characterization for data for compound **17** was obtained controlling the conversion of compound **15** to obtain samples with only one side-product at a time (**14** or **16**).*

*A typical procedure for the generation of **17** in CD_2Cl_2 is described here*. Boramidinate **11** (40 mg, 0.037 mmol) was dissolved in CD_2Cl_2 (1 mL) and placed in a valved NMR tube. The solution was freeze-pump-thawed 3 times and refilled with 1 atm of CO_2. The tube was placed in a rocking platform and reaction progress was followed by NMR until the desired conversion to boramidinate **15** was achieved. The NMR tube was degassed and refilled with 1 atm of CO to generate compound **17** in quantitative yield based on **15**. **^{1}H-NMR** (500 MHz, Methylene Chloride-d_2) δ 8.92 (s, 1H, N-C(*H*)=N), 8.72 (s, 1H, N-C(*H*)=N), 4.43 (t, *J* = 2.0 Hz, 2H, Cp-*H*), 4.22 (t, *J* = 2.0 Hz, 2H, Cp-*H*), 4.03 (t, *J* = 1.8 Hz, 2H, Cp-*H*), 3.80 (t, *J* = 2.0 Hz, 2H, Cp-*H*), 1.63 (s, 9H, -C(CH_3)$_3$), 1.58 (s, 9H, -C(CH_3)$_3$). **^{13}C-NMR** (126 MHz, Methylene Chloride-d_2) partial, δ 159.1 (N-*C*(H)=N), 156.7 (N-*C*(H)=N), 145.8 (N-(*C*O)-O-B), 102.3 (Cp-*C*-N), 99.3 (Cp-*C*-N), 69.6 (Cp-*C*H), 68.8 (Cp-*C*H), 66.9 (Cp-*C*H), 63.0 (Cp-*C*H), 62.9 (-*C*(CH$_3$)$_3$), 58.3 (-*C*(CH$_3$)$_3$), 29.5 (-C(*C*H$_3$)$_3$), 28.5 (-C(*C*H$_3$)$_3$). **^{19}F-NMR** (376 MHz, Methylene Chloride-d_2) partial, δ -131.1 (dd, *J* = 23.6, 8.5 Hz, o-*F*), -134.5 (dd, *J* = 23.4, 9.0 Hz, o-*F*), -154.7 (t, *J* = 20.2 Hz, p-*F*), -155.3 (t, *J* = 20.2 Hz, p-*F*). **^{11}B-NMR** (128 MHz, Methylene Chloride-d_2) δ 0.21, -11.0. **HRMS** (ESI): m/z calcd. $C_{47}H_{29}B_2F_{20}FeN_4O_5^-$ 1187.1376 [M+HCOO]$^-$; found: 1187.1395.

Compound 18 [$C_{54}H_{46}N_6B_2F_{20}Fe$] Compound **11** (25 mg, 23 mmol) was dissolved in dichloromethane (1 mL), *t*-butylisocyanide (100 µL, excess) was added causing an immediate color change from orange to yellow. The solvent was evaporated under reduced pressure, the yellow crystalline residue washed with pentane (1 mL) and dried under vacuum to obtain compound **18**. Yield (19 mg, 66%). **^{1}H-NMR** (500 MHz, Methylene Chloride-d_2) δ 8.52 (s, 2H, N-C(*H*)=N), 4.04 (t, *J* = 2.0 Hz, 4H, Cp-*H*), 3.86 (t, *J* = 1.9 Hz, 4H, Cp-*H*), 1.67 (s, 18H, -C(CH_3)$_3$), 0.94 (s, 18H, -C(CH_3)$_3$). **^{13}C-NMR** (126 MHz, Methylene Chloride-d_2) δ partial, 159.6 (N-*C*(H)=N), 149.8 (br, Aryl-*C*-F), 147.8 (br, Aryl-*C*-F), 141.3 (br, Aryl-*C*-F), 139.4 (br, Aryl-*C*-F), 138.5 (br, Aryl-*C*-F), 136.6 (br, Aryl-*C*-F), 100.3 (Cp-*C*-N), 67.6 (Cp-*C*H), 67.4 (Cp-*C*H), 58.5 (-*C*(CH$_3$)$_3$), 55.9 (-*C*(CH$_3$)$_3$), 30.2 (-C(*C*H$_3$)$_3$), 29.1 (-C(*C*H$_3$)$_3$). **^{19}F-NMR** (376 MHz, Methylene Chloride-d_2) δ -128.6 (br, o-*F*), -156.9 (t, *J* = 20.4 Hz, p-*F*), -163.4 (td, *J* = 22.8, 7.6 Hz, m-*F*). **^{11}B-NMR** (128 MHz, Methylene Chloride-d_2) δ -9.79. FT-IR (ATR, cm^{-1}) 2966, 1678, 1643, 1602, 1515, 1491, 1467, 1454, 1426, 1388, 1362, 1285, 1223, 1202, 1123, 1092, 1028, 1003, 969, 937, 872, 823, 804, 788, 766, 753, 743, 732, 700, 672, 643, 625, 6001, 576, 569, 518, 501, 478, 460, 436. **HRMS** (ESI): m/z calcd. $C_{55}H_{47}B_2F_{20}FeN_6O_2^-$ 1281.3001 [M+HCOO]$^-$; found: 1281.2990. **Elemental Analysis** Experimental C, 52.17; H, 3.99; N, 6.73. Calc. for [$C_{54}H_{46}B_2F_{20}FeN_6$]: C, 52.46; H, 3.75; N, 6.80. **Melting Point**: 179 °C (gas evolution).

Compound 19 [$C_{50}H_{37}N_5B_2F_{20}O_2Fe$] Compound **11** (50 mg, 47 mmol) was dissolved in CD_2Cl_2 (1 mL) and placed in a valved NMR tube. The solution was subjected to 3 freeze-pump-thaw cycles and refilled with 1 atm of CO_2. The tube was tumbled in a rocking table and the conversion was monitored overtime. The reaction was stopped at approximately 65% conversion to boramidinate **15** by degassing the CO_2. The tube was brought into a glovebox and *t*-butylisocyanide (CNtBu) (100 µl, excess) was added causing a color change from dark

orange to orange. The composition of the sample was checked again by NMR. In the glovebox, the solution was evaporated to dryness and $CDCl_3$ (0.75 mL) was added, and the resulting suspension was stirred for 1.5 h. The supernatant was removed, and the resulting orange solid was washed with $CDCl_3$ (2 x 0.25 mL) followed by drying under vacuum. The title compound was obtained as an orange powder in acceptable purity for subsequent analysis (typically 85-95%). (Yield based on **15**: 3 mg, 8%). **^{1}H-NMR** (500 MHz, Methylene Chloride-d_2) δ 8.95 (s, 1H, N-C(*H*)=N), 8.50 (s, 1H, N-C(*H*)=N), 4.24(br, *J* = 1.9 Hz, 2H, Cp-C*H*), 4.13 (t, *J* = 1.9 Hz, 2H, Cp-C*H*), 4.09 (t, *J* = 1.9 Hz, 2H, Cp-C*H*), 3.98 (br, *J* = 1.9 Hz, 2H, Cp-C*H*), 1.69 (s, 9H, -C(CH_3)$_3$), 1.62 (s, 9H, -C(CH_3)$_3$), 0.95 (s, 9H, -C(CH_3)$_3$). **^{13}C-NMR** (126 MHz, Methylene Chloride-d_2) δ partial 159.2 (N-*C*(H)=N), 157.4 (N-*C*(H)=N), 146.02 (N-(*C*O)-O-B), 102.4 (Cp-*C*-N), 100.8 (Cp-*C*-N), 68.9 (Cp-*C*H), 67.9 (Cp-*C*H), 67.3 (Cp-*C*H), 67.0 (Cp-*C*H), 62.8 (-*C*(CH_3)$_3$), 58.7 (-*C*(CH_3)$_3$), 55.9 (-*C*(CH_3)$_3$), 30.2 (-C(*C*H_3)$_3$), 29.4 (-C(*C*H_3)$_3$), 29.2 (-C(*C*H_3)$_3$). **^{19}F-NMR** (376 MHz, Methylene Chloride-d_2) δ 129.6 (br, o-*F*), -135.5 (dd, *J* = 23.0, 9.2 Hz), -156.0 (t, *J* = 20.3 Hz, p-*F*), -157.8 (t, *J* = 20.3 Hz, p-*F*), -163.6 (td, *J* = 23.0, 20.2, 9.3 Hz, m-*F*), -164.4 (td, *J* = 23.4, 22.9, 7.8 Hz, m-*F*). **^{11}B-NMR** (128 MHz, Methylene Chloride-d_2) δ 0.22, -9.81. **FT-IR** (ATR, cm^{-1}) 2976, 1751, 1640, 1608, 1518, 1460, 1375, 1328, 1278, 1224, 1190, 1098, 1033, 968, 940, 925, 872, 831, 790, 778, 753, 737, 705, 686, 671, 644, 600, 577, 501, 486, 471, 446, 427. **HRMS** (ESI): m/z calcd. $C_{50}H_{38}B_2F_{20}FeN_5O_2^-$ 1242.2163 $[M+HCOO]^-$; found: 1242.2155.

Conclusions

We have demonstrated that a molecule bearing two FLP moieties in close proximity can capture different small molecules in a sequential manner. The 1,1'-bis(boramidinate)ferrocene design proved an effective model to study the reactivity of multi-FLP systems which can be further tailored by changing the nature of the carbodiimide substituents or the borane. These findings open the way to design more efficient multi-FLP systems where reactivity can be controlled by the nature of the small molecule and external stimuli (pressure, temperature, conformational changes).

Conflicts of interest

There are no conflicts to declare.

Acknowledgements

This work was funded by a Welch Foundation Grant (F-816). The project that gave rise to these results received financial support of the "la Caixa" Banking Foundation (LCF/BQ/AA17/11610005) in the form of a fellowship for O.E.P. The acquisition of instrument Bruker Avance III HD 400 MHz was made possible by National Science Foundation grant (CHE-1626211). We thank Professor Michael J. Rose for a sample of ^{13}C carbon monoxide.

Notes and references

1 Q. Zhao, R. D. Dewhurst, H. Braunschweig and X. Chen, *Angew. Chemie - Int. Ed.*, 2019, **58**, 3268–3278.
2 D. W. Stephan and G. Erker, *Angew. Chemie - Int. Ed.*, 2015, **54**, 6400–6441.
3 D. W. Stephan, *Acc. Chem. Res.*, 2015, **48**, 306–316.
4 D. W. Stephan, *Science,* 2016, **80**, 354.
5 D. M. Mercea, M. G. Howlett, A. D. Piascik, D. J. Scott, A. Steven, A. E. Ashley and M. J. Fuchter, *Chem. Commun.*, 2019, **55**, 7077–7080.
6 D. H. A. Boom, A. R. Jupp and J. C. Slootweg, *Chem. - A Eur. J.*, 2019, **25**, 9133–9152.
7 Y. Hoshimoto, T. Kinoshita, S. Hazra, M. Ohashi and S. Ogoshi, *J. Am. Chem. Soc.*, 2018, **140**, 7292–7300.
8 D. J. Parks and W. E. Piers, *J. Am. Chem. Soc.*, 1996, **118**, 9440–9441.
9 A. Tlili, A. Voituriez, A. Marinetti, P. Thuéry and T. Cantat, *Chem. Commun.*, 2016, **52**, 7553–7555.
10 J. R. Lawson and R. L. Melen, *Inorg. Chem.*, 2017, **56**, 8627–8643.
11 T. Wang and D. W. Stephan, *Chem. Commun.*, 2014, **50**, 7007–7010.
12 K. L. Bamford, S. S. Chitnis, Z. wang Qu and D. W. Stephan, *Chem. - A Eur. J.*, 2018, **24**, 16014–16018.
13 M.-A. Légaré, G. Bélanger-Chabot, R. D. Dewhurst, E. Welz, I. Krummenacher, B. Engels and H. Braunschweig, *Science*, 2018, **359**, 896–900.
14 R. L. Melen, *Angew. Chemie - Int. Ed.*, 2018, **57**, 880–882.
15 L. Chen, R. Liu and Q. Yan, *Angew. Chemie - Int. Ed.*, 2018, **57**, 9336–9340.
16 M. Wang, F. Nudelman, R. R. Matthes and M. P. Shaver, *J. Am. Chem. Soc.*, 2017, **139**, 14232–14236.
17 Q. Wang, W. Zhao, S. Zhang, J. He, Y. Zhang and E. Y. X. Chen, *ACS Catal.*, 2018, **8**, 3571–3578.
18 L. Wang, D. Deng, K. Škoch, C. G. Daniliuc, G. Kehr and G. Erker, *Organometallics*, 2019, **38**, 1897–1902.
19 X. Jie, Q. Sun, C. G. Daniliuc, R. Knitsch, M. R. Hansen, H. Eckert, G. Kehr and G. Erker, *Chem. – A Eur. J.*, 2020, **26**, 1269–1273.
20 L. Wang, S. Dong, C. G. Daniliuc, L. Liu, S. Grimme, R. Knitsch, H. Eckert, M. R. Hansen, G. Kehr and G. Erker, *Chem. Sci.*, 2018, **9**, 1544–1550.
21 L. Wang, J. Li, D. Deng, C. G. Daniliuc, C. Mück-Lichtenfeld, G. Kehr and G. Erker, *Dalt. Trans.*, 2019, **48**, 11921–11926.
22 J. Li, C. G. Daniliuc, C. Mück-Lichtenfeld, G. Kehr and G. Erker, *Angew. Chemie Int. Ed.*, 2019, **413**, 15377–15380.
23 X. Tao, G. Kehr, C. G. Daniliuc and G. Erker, *Angew. Chemie - Int. Ed.*, 2017, **56**, 1376–1380.
24 A. R. Jupp and D. W. Stephan, *Trends Chem.*, 2019, **1**, 35–48.
25 G. Kehr and G. Erker, *Chem. Rec.*, 2017, **17**, 803–815.
26 Y. Soltani, L. C. Wilkins and R. L. Melen, *Angew. Chemie - Int. Ed.*, 2017, **56**, 11995–11999.
27 M. Santi, D. M. C. Ould, J. Wenz, Y. Soltani, R. L. Melen and T. Wirth, *Angew. Chemie - Int. Ed.*, 2019, **58**, 7861–7865.
28 A. Berkefeld, W. E. Piers and M. Parvez, *J. Am. Chem. Soc.*, 2010, **132**, 10660–10661.
29 M. Bakos, Á. Gyömöre, A. Domján and T. Soós, *Angew.*

Chemie - Int. Ed., 2017, **56**, 5217–5221.
30 T. Mahdi and D. W. Stephan, *Angew. Chemie - Int. Ed.*, 2015, **54**, 8511–8514.
31 E. A. Romero, T. Zhao, R. Nakano, X. Hu, Y. Wu, R. Jazzar and G. Bertrand, *Nat. Catal.*, 2018, **1**, 743–747.
32 D. W. Beh, W. E. Piers, B. S. Gelfand and J. Lin, *Dalton Trans.*, 2020, **49**, 95-101.
33 T. Matsuo and H. Kawaguchi, *J. Am. Chem. Soc.*, 2006, **128**, 12362–12363.
34 J. Bauer, H. Braunschweig and R. D. Dewhurst, *Chem. Rev.*, 2012, **112**, 4329–4346.
35 N. P. Mankad, *Chem. Commun.*, 2018, **54**, 1291–1302.
36 N. P. Mankad, *Chem. - A Eur. J.*, 2016, **22**, 5822–5829.
37 J. Campos, *J. Am. Chem. Soc.*, 2017, **139**, 2944–2947.
38 N. Hidalgo, C. Maya and J. Campos, *Chem. Commun.*, 2019, **55**, 8812–8815.
39 N. Hidalgo, S. Bajo, J. J. Moreno, C. Navarro-Gilabert, B. Q. Mercado and J. Campos, *Dalt. Trans.*, 2019, **48**, 9127–9138.
40 O. Esarte Palomero and R. A. Jones, *Organometallics*, 2019, **38**, 2689–2698.
41 R. Boese, R. Köster and M. Yalpani, *Zeitschrift für Naturforsch. B*, 1994, **49**, 1453–1458.
42 M. A. Dureen and D. W. Stephan, *J. Am. Chem. Soc.*, 2010, **132**, 13559–13568.
43 M. Ríos-Gutiérrez, L. R. Domingo, R. S. Rojas, A. Toro-Labbé and P. Pérez, *Dalt. Trans.*, 2019, **48**, 9214–9224.
44 A. Ramos, A. Antiñolo, F. Carrillo-Hermosilla, R. Fernández-Galán, M. D. P. Montero-Rama, E. Villaseñor, A. Rodríguez-Diéguez and D. García-Vivó, *Dalt. Trans.*, 2017, **46**, 10281–10299.
45 C. Das Neves Gomes, E. Blondiaux, P. Thuéry and T. Cantat, *Chem. - A Eur. J.*, 2014, **20**, 7098–7106.
46 A. Ramos, A. Antiñolo, F. Carrillo-Hermosilla, R. Fernández-Galán and D. García-Vivó, *Chem. Commun.*, 2019, **55**, 3073–3076.
47 M. A. Légaré, M. A. Courtemanche and F. G. Fontaine, *Chem. Commun.*, 2014, **50**, 11362–11365.
48 A. Adenot, N. von Wolff, G. Lefèvre, J. C. Berthet, P. Thuéry and T. Cantat, *Chem. - A Eur. J.*, 2019, **25**, 8118–8126.
49 S. Moreno, A. Ramos, F. Carrillo-Hermosilla, A. Rodríguez-Diéguez, D. García-Vivó, R. Fernández-Galán and A. Antiñolo, *Inorg. Chem.*, 2018, **57**, 8404–8413.
50 A. Ramos, A. Antiñolo, F. Carrillo-Hermosilla, R. Fernández-Galán, A. Rodríguez-Diéguez and D. García-Vivó, *Chem. Commun.*, 2018, **54**, 4700–4703.
51 A. R. Cabrera, R. S. Rojas, M. Valderrama, P. Plüss, H. Berke, C. G. Daniliuc, G. Kehr and G. Erker, *Dalt. Trans.*, 2015, **44**, 19606–19614.
52 A. Antiñolo, F. Carrillo-Hermosilla, R. Fernández-Galán, J. Martínez-Ferrer, C. Alonso-Moreno, I. Bravo, S. Moreno-Blázquez, M. Salgado, E. Villaseñor and J. Albaladejo, *Dalt. Trans.*, 2016, **45**, 10717–10729.
53 Unpublished results.
54 D. J. Parks, W. E. Piers and G. P. A. Yap, *Organometallics*, 1998, **17**, 5492–5503.
55 E. A. Patrick and W. E. Piers, *Chem. Commun.*, 2020, **56**, 841–853.
56 I. B. Sivaev and V. I. Bregadze, *Coord. Chem. Rev.*, 2014, **270–271**, 75–88.
57 X. Li, C. Ni, H. Song and C. Cui, *Chem. Commun.*, 2006, 1763–1765.
58 G. W. Margulieux, N. Weidemann, D. C. Lacy, C. E. Moore, A. L. Rheingold and J. S. Figueroa, *J. Am. Chem. Soc.*, 2010, **132**, 5033–5035.
59 A. Preuß, M. Korb, D. Miesel, T. Rüffer, A. Hildebrandt and H. Lang, *Dalt. Trans.*, 2019, **48**, 14418–14432.
60 L. E. Longobardi, T. C. Johnstone, R. L. Falconer, C. A. Russell and D. W. Stephan, *Chem. - A Eur. J.*, 2016, **22**, 12665–12669.
61 J. A. Soderquist and A. Negron, *Org. Synth.*, 2003, 169–169.